



## Cone-beam micro computed tomography dedicated to the breast



Antonio Sarno<sup>a,b,\*</sup>, Giovanni Mettivier<sup>a,b</sup>, Francesca Di Lillo<sup>a,b</sup>, Mario Cesarelli<sup>c</sup>,  
Paolo Bifulco<sup>c</sup>, Paolo Russo<sup>a,b</sup>

<sup>a</sup> Dipartimento di Fisica "Ettore Pancini", Università di Napoli Federico II, Complesso Universitario di Monte Sant' Angelo, Via Cintia, snc, I-80126 Napoli, Italy

<sup>b</sup> Istituto Nazionale di Fisica Nucleare, Sezione di Napoli, I-80126 Napoli, Italy

<sup>c</sup> Dipartimento di Ingegneria Elettrica e Tecnologie dell'Informazione, Università di Napoli Federico II, I-80125 Napoli, Italy

### ARTICLE INFO

#### Article history:

Received 10 March 2016

Revised 23 August 2016

Accepted 23 September 2016

#### Keyword:

Breast cancer

Diagnosis

Micro computed tomography

Phase contrast

MTF

### ABSTRACT

We developed a scanner for micro computed tomography dedicated to the breast (B<sub>μ</sub>CT) with a high resolution flat-panel detector and a microfocus X-ray tube. We evaluated the system spatial resolution via the 3D modulation transfer function (MTF). In addition to conventional absorption-based X-ray imaging, such a prototype showed capabilities for propagation-based phase-contrast and related edge enhancement effects in 3D imaging. The system limiting spatial resolution is 6.2 mm<sup>-1</sup> (MTF at 10%) in the vertical direction and 3.8 mm<sup>-1</sup> in the radial direction, values which compare favorably with the spatial resolution reached by mini focus breast CT scanners of other groups. The B<sub>μ</sub>CT scanner was able to detect both microcalcification clusters and masses in an anthropomorphic breast phantom at a dose comparable to that of two-view mammography. The use of a breast holder is proposed in order to have 1–2 min long scan times without breast motion artifacts.

© 2016 IPEM. Published by Elsevier Ltd. All rights reserved.

### 1. Introduction

Computed tomography (CT) dedicated to the breast (breast CT, BCT) is an X-ray imaging technique that produces 3D images of the breast anatomy for breast cancer diagnosis. It features an isotropic resolution and absence of breast compression, the latter causing discomfort to the patients in mammographic exams as well as in digital breast tomosynthesis scans [1–3]. A recent review was provided by Sarno et al. [2]. BCT, introduced in 2001 [1,3] is able to overcome the well-known limits of mammography due to the superposition of the tissues, which may hide tumor masses and hence may reduce sensitivity.

In a BCT exam, the patient, lying on a table in prone position, inserts her breast in a hole in the bed and the breast, hanging freely from the hole, is imaged via an X-ray tube and a flat panel detector: the gantry rotates under the table in the coronal plane [1–3]. X-ray tube voltages from 49 to 80 kVp are routinely adopted in BCT setups. The prototype developed at University of Rochester and produced by a spinoff company [3–5] received FDA approval for diagnostic imaging of the breast in conjunction with standard two-view mammography [6], as well as the CE mark. The

dose delivered to the breast during the imaging session via such a commercial scanner was estimated to be from 1.4 to 7.2 times higher than that used in 2-views mammography exams for the same breast [7].

A limit of first-generation BCT scanners is their relatively low spatial resolution, which ranges between 1.7 mm<sup>-1</sup> and 5.6 mm<sup>-1</sup>, when evaluated as the spatial frequency at which the modulation transfer function (MTF) curve reaches 10% (MTF<sub>0.1</sub>) [1]. For comparison, the limiting resolution of full-field digital mammography (FFDM) reaches 12 mm<sup>-1</sup> [8]. This relatively low spatial resolution might present problems for the BCT performance in detecting microcalcification clusters. In clinical studies, the BCT systems developed at University of Rochester [5] and at University of California Davis [9] detected 84.8% and 66.7% of the microcalcification clusters embodied in the imaged breast, respectively. Several factors limit the maximum BCT system spatial resolution: (i) the penumbra caused by the large size of the focal spot of the X-ray source (typically in the order of 0.3–0.4 mm nominal), (ii) the relatively large flat-panel detector pixel pitch (typically about 0.2 mm), (iii) the blurring introduced by the gantry motion, and (iv) the scintillator layer of the flat panel detector, usually thicker than that adopted in FFDM, for the need to detect more penetrating photons than in mammography. Many efforts have been made to reduce the influence of these limiting factors. The group at the University of Rochester developed a BCT scanner with a pulsed X-ray source in order to reduce gantry motion influence on the system spatial

\* Corresponding author at: Dipartimento di Fisica "Ettore Pancini", Università di Napoli Federico II, Complesso Universitario di Monte Sant' Angelo, Via Cintia, snc, I-80126 Napoli, Italy.

E-mail address: [sarno@na.infn.it](mailto:sarno@na.infn.it) (A. Sarno).

resolution, which reached  $1.9 \text{ mm}^{-1}$  [4]. The group at UC Davis improved the spatial resolution of its BCT prototype by embodying in the setup a pulsed X-ray tube and a high resolution CMOS flat panel detector with a pixel pitch of  $75 \mu\text{m}$  (which works with an effective pixel pitch of  $150 \mu\text{m}$ ) coupled to a thin CsI(Tl) scintillator layer [10]. Thanks to these upgrades, the limiting spatial resolution of the first two prototypes, lower than  $1.8 \text{ mm}^{-1}$  [11], increased up to  $3.6 \text{ mm}^{-1}$  for the fourth prototype at UC Davis [12]. The high-resolution, direct-conversion, CdTe photon counting detector allowed the spiral BCT scanner developed at Erlangen University to reach a spatial resolution up to  $5.3 \text{ mm}^{-1}$  [13]. This gives the potential of showing microcalcifications with a diameter down to  $150 \mu\text{m}$  [14,15].

Our group at the Department of Physics at University of Naples Federico II developed a first scanner for micro CT dedicated to the breast ( $B_{\mu}\text{CT}$ ). It embodied a high resolution CMOS flat panel detector with a pixel pitch of  $50 \mu\text{m}$  and a  $150\text{-}\mu\text{m}$  thick CsI(Tl) scintillator layer, and an X-ray source with a micro focal spot of  $40 \mu\text{m}$  nominal size [16]. That prototype reached a limiting spatial resolution of  $3 \text{ mm}^{-1}$  [16]. The effective detector pixel pitch, the focal spot size and the spatial resolution of the prototypes developed at UC Davis, U Rochester, U Erlangen and U Naples are summarized in Table A1 (in Appendix). This work presents the characterization of the new  $B_{\mu}\text{CT}$  scanner developed at U Naples (third prototype, Table A1): here, the X-ray tube has been replaced with a micro focal spot ( $7 \mu\text{m}$ ) tube. In this work, the system MTF is described and the 1D noise power spectra (NPS) have been evaluated.

When an X-ray e.m. wave passes through an object, both its amplitude and phase change. Using phase-detection techniques, the spatially-resolved phase shift of the X-ray wave can be detected in a plane transverse to the beam axis. Soft tissues, which present small differences in attenuation coefficients as in the case of certain types of breast lesions and healthy tissues, can present larger differences in the emerging X-ray beam phase shift. Propagation-based phase contrast imaging (PB-PhC) is an imaging technique that does not need special optical elements in the beam path, apart from an X-ray incident beam with some degree of spatial coherence and a sufficient distance between the imaged object and the detector. It can be implemented either with synchrotron radiation sources [17,18,19] or in the laboratory using compact micro-focus X-ray tubes [20]. The advantages of the edge enhancement effects in projected images in PB-PhC [21,22] – produced by X-ray refraction at the boundary of different tissue structures – have already been shown in FFDM [23,24]. The micro-focal spot of the new scanner developed at U Naples, together with a sufficient distance between source and imaged object, produces an X-ray beam with sufficient spatial coherence, which makes this  $B_{\mu}\text{CT}$  scanner a viable tool for PB-PhC for future clinical applications. In this work, the edge enhancement produced by the phase effects, both in planar and in 3D reconstructed images, was investigated.

A phantom study was conducted in order to test the capability of the  $B_{\mu}\text{CT}$  scanner in showing phantom microcalcifications and soft tissue lesions with a dose similar to the one used in two-views FFDM and with a long scan time still considered adequate for in clinical use.

## 2. Materials and methods

### 2.1. The cone beam $B_{\mu}\text{CT}$ system

The cone-beam microCT scanner dedicated to the breast (Fig. 1) is a modular benchtop system, which embodies the components described below.

(1) A 75-W microfocus X-ray tube (Hamamatsu model L8121-03) with a selectable focal spot whose size of 7, 20 or  $50 \mu\text{m}$ . This

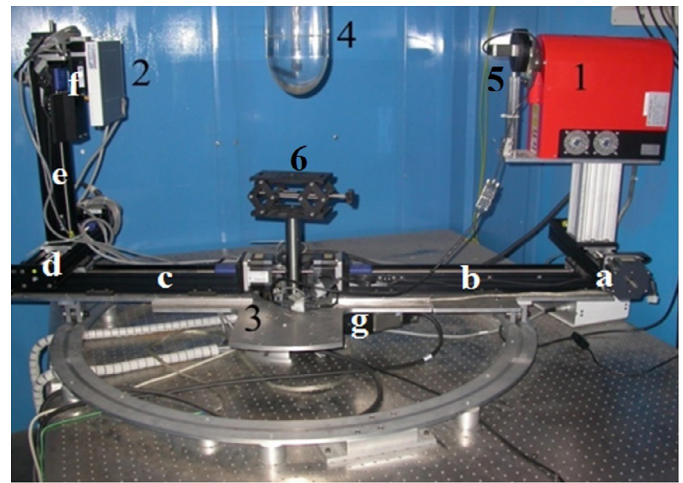


**Fig. 1.** Cone-beam microCT prototype scanner dedicated to breast imaging. (1) Microfocus X-ray tube and (2) CMOS flat panel detector, mounted on step-motor linear stages for variable-magnification imaging; (3) step-motor rotating gantry; (4) hanging PMMA breast phantom placed at isocenter and simulating a pendant breast; (5) rotating filter wheel for beam shutter; (6) post and lab jack at isocenter for hosting phantoms. Step-motor linear stages (a–e) and rotation stages (f, g) are used for setting the acquisition geometry and for gantry rotation. The system is mounted on an optical table ( $1.8 \text{ m} \times 1.2 \text{ m}$ ) and the patient bed can be positioned at  $154 \text{ cm}$  from the floor.

air-cooled tube has a fixed tungsten anode, a cone angle of  $43^\circ$  and it can be operated at a constant voltage between  $40 \text{ kV}$  and  $150 \text{ kV}$ ; the output window is made of  $0.2\text{-mm}$  Be and the added filtration is  $1.58 \text{ mm}$  Al. The measured half value layer (HVL) at  $50 \text{ kV}$  is  $1.3 \text{ mm}$  Al. The distance between source and isocenter is  $612 \text{ mm}$ . Fig. A1 (in Appendix) shows the tube output at isocenter as a function of tube voltage. Table 1 shows the scan time necessary to deliver a mean glandular dose (MGD) of  $4 \text{ mGy}$  to a  $14\text{-cm}$  diameter and  $50\%$  glandular breast, calculated on the basis of the tube output at isocenter and on the basis of the monoenergetic normalized glandular dose (DgN) coefficients evaluated by Thacker and Glick [25]. The X-ray spectra were simulated with SpekCalc [26]. The duration of a full  $360^\circ$  scan is in the range of  $69 \text{ s}$  (@  $120 \text{ kV}$ ) to  $336 \text{ s}$  (@  $40 \text{ kV}$ ) when the focal spot is set to  $7 \mu\text{m}$ , decreasing correspondingly to  $11\text{--}161 \text{ s}$  with a  $50\text{-}\mu\text{m}$  focal spot. Hence, scans in which the patient is holding her breath are not feasible, and patient specific tools capable of immobilizing the breast during the scan are necessary.

(2) A CMOS flat panel detector (Hamamatsu mod. C7942CA-02) with a  $150\text{-}\mu\text{m}$  thick CsI:Tl scintillator layer, with a sensitive area of  $12 \text{ cm} \times 12 \text{ cm}$  and a  $50\text{-}\mu\text{m}$  pixel pitch. According to specifications, the C7942CA detector has a spatial resolution of  $8 \text{ lp/mm}$  (at  $5\%$  Contrast Transfer Function); the measured MTF reaches  $10\%$  at  $6 \text{ mm}^{-1}$  [16]. The detective quantum efficiency of the detector is higher than  $0.4$  at zero frequency (at  $60 \text{ kVp}$ , mean energy =  $36.3 \text{ keV}$ ) [27]. The frame rate is  $2 \text{ fps}$  at  $1 \times 1$  pixel binning ( $2.13 \text{ fps}$  measured rate),  $4 \text{ fps}$  at  $2 \times 2$  binning and  $9 \text{ fps}$  at  $4 \times 4$  binning. The analog-to-digital conversion produces  $12 \text{ bit/pixel}$  signals in analog to digital units (ADU). Fig. A2a (in Appendix) shows the results of a test for assessing the detector lag, confirming the limited relevance of this effect for the CMOS flat panel detector.

We acquired four hundred consecutive frames and then calculated the average pixel value in a  $400 \times 400$  pixels region of interest (ROI). The curves for  $50$ ,  $80$  and  $100 \text{ kV}$  were normalized to their starting values. The results showed a weak upward trend where the mean signal increases up to  $0.7\%$  (at  $80 \text{ kV}$ ) from its starting value after  $400$  consecutive projections. Previous studies [28] showed an asymptotic trend for this curve. Fig. A2b (in Appendix) shows linearity of detector signal (evaluated as the mean

Download English Version:

<https://daneshyari.com/en/article/5032775>

Download Persian Version:

<https://daneshyari.com/article/5032775>

[Daneshyari.com](https://daneshyari.com)